1974

Calculation and Measurement of the Crankshaft Motion In the Bearings of a Refrigeration Compressor

H. Kruse
Technical University Hannover

W. Roettger
Technical University Hannover

R. Vauth
Technical University Hannover

CALCULATION AND MEASUREMENT OF THE CRANKSHAFT MOTION IN THE BEARINGS OF A REFRIGERATION COMPRESSOR

Dr. H. Kruse, Professor of Refrigeration Engineering
W. Röttger, Dipl. Ing.
R. Vauth, Dipl. Ing.
Technische Universität Hannover/Germany

Introduction

Radial bearings in reciprocating engines, i.e. in internal combustion engines, compressors,and hydraulic reciprocating engines are dynamically loaded. We have a dynamic load when forces acting on the bearing change periodically in magnitude and direction, and/or when the angular velocity of the shaft, and/or the bearings, are changeable. Among the computing methods that have been developed for the construction of the bearings thus loaded, the computing method of the crankshaft movement in the bearings has found many applications. So far experiences have shown that this method, developed by Hahn [1], Holland [2] and Eberhard-Lang [3], is superior to other methods, as far as accuracy is concerned. Gläser [4] applied this computing method of the crankshaft movement to refrigeration compressors without, however, taking into account the lubrication conditions caused by refrigerant-oil-mixtures.

Computing method of the crankshaft motion

The computing method of the crankshaft movement determines the movement of the journal in the bearing.

At any given point in time the position of the journal is described through the relative eccentricity ε and through the displacement angle of the shaft between the vertical and the smallest lubrication gap.

For the computing, knowledge of the load process per unit time is necessary. The force F acting on the bearing has to be conveyed by the lubrication film. The oil presure is built up, on one hand through the rotary motion of the journal and/or of the bearing, and on the other hand through the radial motion of the journal. The load F_D

$$F_D = \frac{So_D \cdot b \cdot d \cdot \eta \cdot \bar{\omega}}{\psi^2} \qquad (1)$$

through rotation only and the load F_V

$$F_V = \frac{So_V \cdot b \cdot d \cdot \eta}{\psi^2} \frac{d\varepsilon}{dt} \qquad (2)$$

through radial motion only, have to be in equilibrium with the outer bearing force F. Fig. 1 shows the force system at the bearing.

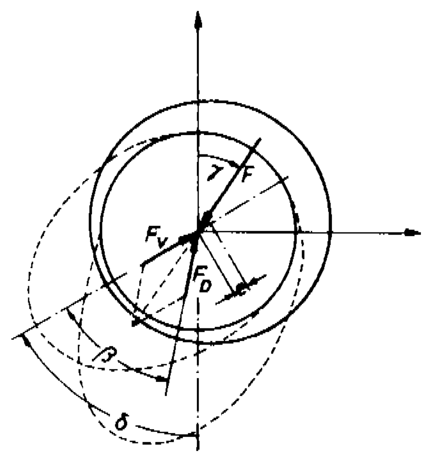

Fig. 1: Force system at the bearing

$\bar{\omega}$ is the effective angular velocity defined by Fränkel [5].

$$\bar{\omega} = \omega + \omega_s - 2\frac{d\delta}{dt} \qquad (3)$$

By inserting the equilibrium of forces in the differential equation of Reynolds, which describes the pressure distribution in the bearing, one gets two differential equations for the determination of the values ε and δ. By transition to finite time steps Δt, expressed through crank angle steps

$$\Delta t = \frac{\Delta\phi}{\omega} \qquad (4)$$

we gain the difference equation

$$\Delta\varepsilon = \frac{\Delta\phi}{\omega} \frac{F \cdot \psi^2}{d \cdot b \cdot \eta \cdot So_V}\left[\cos(\delta-\gamma) - \left|\frac{\sin(\delta-\gamma)}{\tan\beta}\right|\right] \qquad (5)$$

and

$$\Delta\delta = \frac{\Delta\phi}{\omega}\left[\frac{\bar{\omega}}{2} - \frac{F \cdot \psi^2}{d \cdot b \cdot \eta \cdot So_D} \frac{\sin(\delta-\gamma)}{2\sin\beta}\right] \qquad (6)$$

By means of these equations the change of ε and δ between two different crank angle positions is gained. The position of the journal at the end of the time interval is computed by

$$\varepsilon_{i+1} = \varepsilon_i + \Delta\varepsilon \qquad (7)$$

and

$$\delta_{i+1} = \delta_i + \Delta\delta \tag{8}$$

For the computation, the position of the journal must be known at the beginning of the time interval. The computation therefore starts off with estimations of ε_o and δ_o. It is calculated by means of the approxima-tion equations given by Eberhard-Lang [3]. Starting from ε_o and δ_o, the changes $\Delta\varepsilon$ and $\Delta\delta$ can be computed for the first crank angle step. For the values ε_1 and δ_1 so gained, the Sommerfeld-number So_D and So_V and the angle ß are fixed. The computation is exten-ded over the full work cycle and beyond, until the ε and δ values correspond to the previous computation within a required accu-racy. Even with large estimations, the com-putation method converges rapidly, so that the computation may in most cases be stopped after only two circuits.
The load on the bearing consists of gas and inertia forces. The forces due to inertia are ascertained through the knowledge of the mass and acceleration, which result from the rotational speed and the crank assembly geo-metry.
To obtain the gas forces two ways are pos-sible:

1. For the investigation of the crankshaft movement of already existing machines the gas forces can be defined by means of a measured p-v-diagram.
2. Through a mathematical model which takes into account influencing values, the gas forces of a machine under development have to be computed.

<u>Mathematical model for computing the cycle of a refrigeration compressor</u>

The mathematical model, describing the cycle of operation of a high speed positive dis-placement compressor, is based on the First Law of Thermodynamics

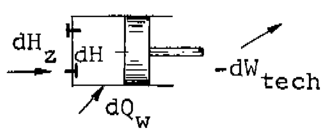

$$dH = dQ_w + Vdp + dH_z \tag{9}$$

Terms of potential and kinetic energy may be neglected. Through introducing the spe-cific energy values

$$H = m \cdot h \quad (10a) \qquad H_z = m \cdot h_z \quad (10b)$$

and the term describing heat transfer

$$dQ_w = \Sigma\alpha_i A_{wi}(T_{wi} - T)dt \tag{11}$$

and

$$\phi = \omega \cdot t \tag{12}$$

we gain the equation for the derivation of the specific enthalpy with regard to the crank angle

$$\frac{dh}{d\phi} = \frac{\Sigma\alpha_i A_{wi}(T_{wi} - T)}{m \cdot \omega} + \frac{V}{m}\frac{dp}{d\phi} + \frac{h_z - h}{m}\frac{dm}{d\phi} \tag{13}$$

Thereby z is a generalized index (see appendix).
It is presupposed that the cylinder charge is homogenous, and that the conditions on the suction and discharge cavities are con-stant (i.e. no pulsations in the pipe lines).
By means of the ideal gas law,

$$pV = mRT \tag{14}$$

we easily get the derivation of the cylin-der pressure with respect to the crank an-gle

$$\frac{dp}{d\phi} = \frac{RT}{V}\frac{dm}{d\phi} - \frac{mRT}{V^2}\frac{dV}{d\phi} + \frac{mR}{V}\frac{dT}{d\phi} \tag{15}$$

With the knowledge of the temperature de-pendency on the specific heat of an ideal gas at a constant pressure [8] we have for the enthalpy

$$h - h_o = \int_{T_o}^{T} c_p(t)\, dT \tag{16}$$

and thereby for the derivation of the en-thalpy with respect to the crank angle:

$$\frac{dh}{d\phi} = c_p(T) \cdot \frac{dT}{d\phi} \tag{17}$$

From the equations (13), (15) and (17) we get the differential equation for the tem-perature:

$$\frac{dT}{d\phi} = \frac{1}{c_p(T) - R}\left\{\frac{\Sigma\alpha_i A_{wi}(T_{wi} - T)}{m \cdot \omega} - \frac{RT}{V}\frac{dV}{d\phi} + \left[RT + \int_{T}^{T_z} c_p(T)dT\right]\frac{1}{m}\frac{dm}{d\phi}\right\} \tag{18}$$

For computing the expansion and the com-pression process we have

$$\frac{dm}{d\phi} = 0 \tag{19}$$

The change of the cylinder volume with re-spect to the crank angle is easy to derive from the geometry of the crank assembly:

$$\frac{dV}{d\phi} = \frac{D^3 \cdot \pi}{8}\left[\sin\phi + \frac{\lambda_c \cdot \sin\phi \cdot \cos\phi}{\sqrt{1 - \lambda_c^2 \sin^2\phi}}\right] \tag{20}$$

The heat transfer coefficient can only be estimated. An exact formula, which computes the function of the heat transfer coeffi-cient for all reciprocating engines depen-ding on place and time, is not obtainable because of the great number of influential parameters and because of a lack of know-ledge of the boundary conditions.
Therefore, empirical correlations have been developed for the convective heat transfer with internal combustion engines [9, 10]. These correlations start off from the heat

transfer in the pipe flow and are derived by means of the similarity theorem of Nusselt. For $Pr \neq f(T)$ is

$$Nu = C_A \cdot Re^k \tag{21}$$

With compressors conditions are more favourable than with internal combustion engines, since we can leave out the convective part caused by the combustion. The heat transfer coefficient can be represented in the form

$$\alpha = C_A \cdot \lambda \cdot d^{k-1} \left(\frac{c_m}{\eta \nu} \right)^k \tag{22}$$

Through a distribution of the heat transfer area in zones of different constant wall temperatures, and through a separation of the process into its different phases of time we can obtain a reasonable calculation of the heat transfer coefficient with a great effort. If we neglect in a rough approximation the above mentioned, the heat transfer area with the average wall temperature T_W results in

$$A(\phi) = D \cdot \pi \left\{ \frac{D}{2} + r \left[2\varepsilon_o + (1 - \cos\phi) + \frac{1}{\lambda_c} \left(1 - \sqrt{1 - \lambda_c^2 \sin^2\phi} \right) \right] \right\} \tag{23}$$

With the knowledge of these connections, the compression and expansion processes can be worked out through a step by step integration (e.g. Runge-Kutta-method). Since m, V and T are known, any thermodynamic value of interest, for example: pressure, enthalpy and entropy, can be ascertained.
To compute the suction and discharge process, the mass flow $dm/d\phi$ must be known. If we compare the valve flow with an adiabatic nozzle flow, where we can leave out the kinetic energy upstream, we gain

$$\frac{dm}{d\phi} = \frac{A_{Qeff} p_1}{\omega} \sqrt{\frac{2\kappa}{(\kappa - 1) R T_1} \left[\left(\frac{p_2}{p_1} \right)^{\frac{2}{\kappa}} - \left(\frac{p_2}{p_1} \right)^{\frac{\kappa+1}{\kappa}} \right]} \tag{24}$$

for

$$\frac{p_2}{p_1} > \left(\frac{2}{\kappa + 1} \right)^{\frac{\kappa}{\kappa - 1}} \tag{25}$$

Thereby the effective flow area is a function of the relative valve lift y [11]

$$A_{Qeff}(y) = C_Q(y) \cdot A_Q \tag{26}$$

whereby the flow coefficient C_Q includes the flow losses. If we take into account the influence of the valve dynamics by using a differential equation of second order,

$$FVH^2 \cdot y'' + 2 \cdot DFK \cdot FVH \cdot y' + y + VSP = ERG \cdot x \tag{27}$$

the suction and discharge phase of the cycle process is computable while simultaneously solving the differential equational system consisting of the equations (18), (24) and (27). The loss of kinetic energy of the valve plate on impact, as well as the adhesive effect can be described by a coefficient of restitution and an adhesive coefficient respectively.
If the initial conditions are well estimated, usually two computing operations are enough to gain a sufficient correlation between initial and end values of the cycle process computation.
Finally we may point out that such a mathematical model is semi-analytical. Apart from the geometrical values, the property values, and values of the operation conditions, the knowledge of the following characteristics and functions, obtainable by measurement, has to be presupposed: namely the effective flow area, the effective force area, the damping coefficient, the coefficients of restitution and adhesion as well as the characteristics constants of the heat transfer coefficient correlation.

<u>Crankshaft motion of a main bearing</u>
<u>Measurement of the crankshaft motion</u>

The measurements were executed with a semi-hermetical DWM-Copeland 2-cylinder refrigeration compressor, type DKSJB/100W. Its most important data are:

Performance:	P =	1	PS
Revolutions per minute:	n =	1450	rpm
Cylinder diameter:	D =	39,5	mm
Stroke:	S =	29,4	mm
Cubic capacity:	V_H =	6,33	m^3/h

The investigated main bearing has the following measurements:

Diameter:	d =	22,21	mm
Width:	b =	20,00	mm
Relative bearings clearance:	ψ =	0,00173	

The following values were measured:
1. Crankshaft movements, test points 1 to 4
2. Top center, test points 5 and 6
3. Bearing pressure, test point 7
4. Cylinder pressure with insertion of suction and discharge chamber pressure as well as reference pressures, test point 8
5. Crankcase pressure, testpoint 9
6. Oil and gas temperatures, test points 15 to 24

Fig. 2 shows the refrigeration cycle and the test arrangement.
The pressures were measured with piezo pickups made by Kistler, the paths with contactless inductive pickups made by Hottinger, and the temperatures with coaxial thermoelements.
The measurement of the crankshaft movement had to be executed directly inside the bearing, since for reasons of construction it was impossible to lead the journal through the end plate. To gain a better linearity of the reading, four pickups were coupled to make a differential circuit. Figure 3 shows the arrangement of the test points in the endplate. The pickups had to be calibrated when already built in, because the initial

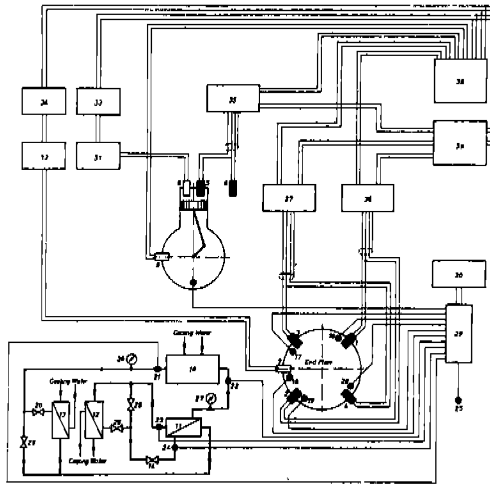

Fig. 2: Refrigeration cycle and test arrangement

air gap had to be kept constant. By means of the calibration jig a journal could be moved in the bearing and thus the calibration could be executed.

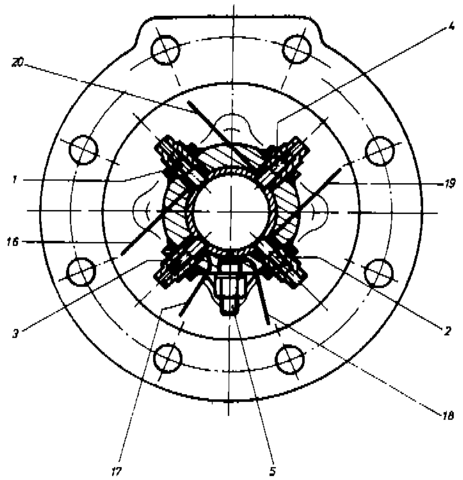

1 - 4 Displacement pickups
5 Pressure pickup
16 - 20 Thermoelements

Fig. 3: Arrangement of test points in endplate

In order to measure the cylinder pressure, an adapter was built, which allowed measurement of the cylinder pressure as well as momentary measurement of the suction chamber, the discharge chamber and a reference pressure, one after the another, by reversing the actuating piston by means of pilot pressure.
Figure 4 shows the actuating piston of the adapter and the reversing system.
The measurement of the bearing temperature served to find out the temperature distribution and to make possible the determination of the viscosity of the oil-refrigerant mixture in the bearing.

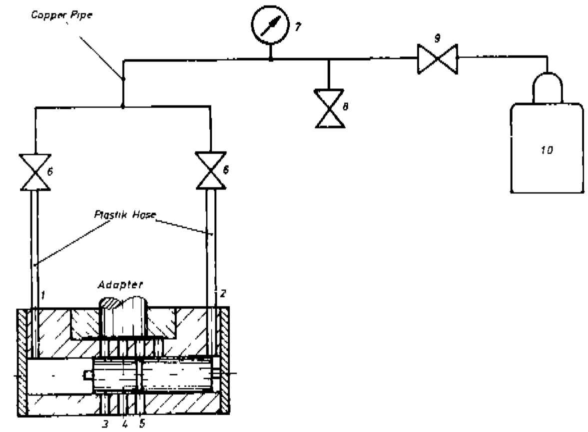

Fig. 4: Reversing device

The aim of the measurements at the compressor was to investigate the influence of the refrigerant dissolved in oil on the lubrication conditions. Therefore the cycle was operated with
1. refrigerant R12
2. refrigerant R502.
For lubrication the refrigeration compressor oil KM made by Fuchs was used in both cases.
R12 is fully mixable with oil while R502 shows only a limited mixability according to Ashrae [7]. When operating the compressor with R502, no or only very little refrigerant was dissolved in oil, since the cycle was operated in such a manner that the refrigerant was in a gaseous state in the whole cycle.
For both modes of operaton (with R12 and R502) the suction and counter pressures were adjusted in such a way that the bearing load caused by the gas forces remained almost the same.

Discussion of the measurement and computation results

The figures 5 to 7 show the measurement results for operating with R12. While the p-v-diagram (fig. 5) of the three measurements show only slight variations, the journal movements (fig. 6) show larger variations.
These variations are caused by the fact that the position of the journal could not be determined when recording the zero line. For the evaluation, it was assumed that the journal, when the aggregate is at standstill, that is, at the time of the zero line recording, was at the lowest point of the bearing. The further consideration presupposes that, for the graph of the second measurement, the above mentioned condition is fulfilled. Through the different paths shown in the measurement, the path motion of the journal (fig. 7) was determined by geometrical addition.
For the cumputed path motions, (also shown in fig. 7) the pressure values of the p-v-diagram of the second measurement had to be fed in, for a crank angle step of 2^{o}.

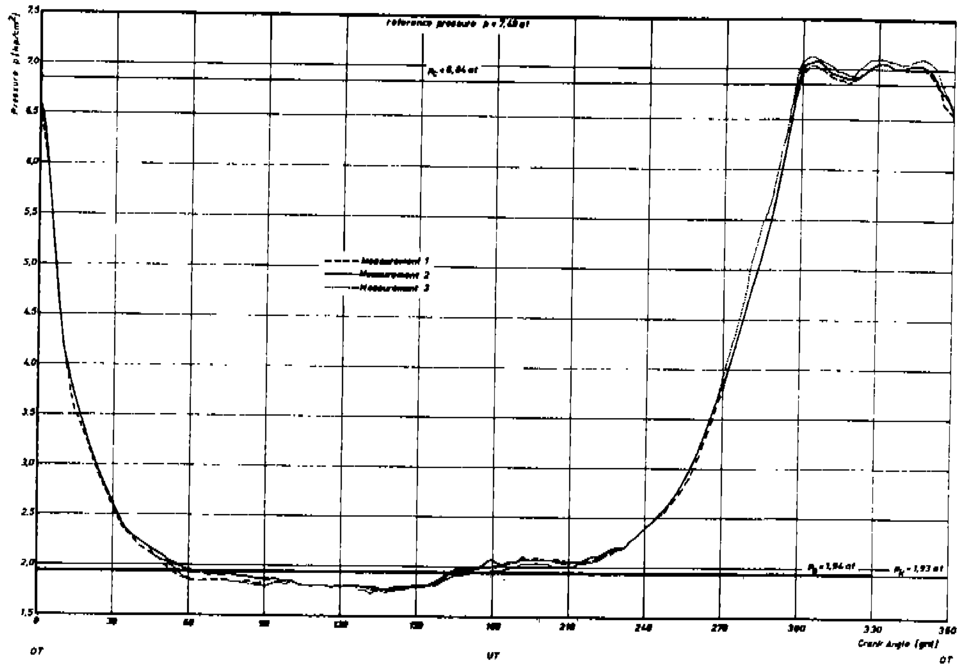

Fig. 5:
Cylinder pressure

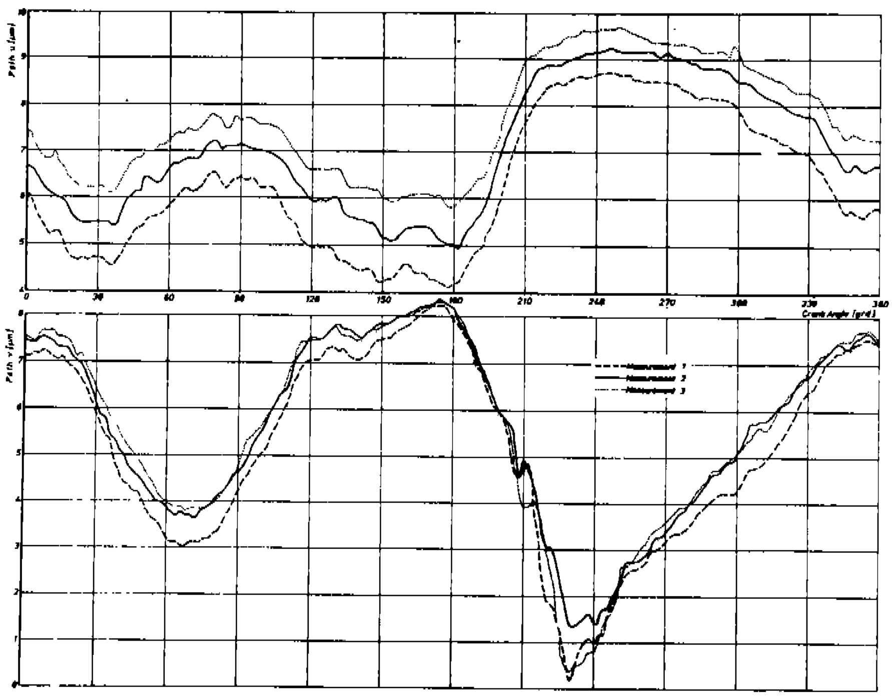

Fig. 6:
Journal movement in x and y direction

The viscosity, obtained from the data of the oilproducer was $\eta = 1.17 \cdot 10^{-7}$ kp s/m^2.
To ascertain the change of the path motion caused by the refrigerant constituent in oil the computation was executed in addition for $\eta = 0{,}95 \cdot 10^{-7}$ and $\eta = 0{,}85 \cdot 10^{-7}$ kp s/m^2.
The path motions show two almost closed paths of the curve. On one hand between 0° and 180° crank angle and on the other between 180° and 360°. Here the influence of the two cylinders, which have a difference of 180°, is shown clearly. In all cases, the path motions follow the changes of the loads, a fact which is clearly shown by the measured path.
The load decrease in the cylinder nearest to the bearing (cylinder 1) causes, at first, an eccentricity decrease. Through the compression of cylinder 2, which starts at about 60° crank angle, the bearing is again loaded, so that the relative eccentricity increases. This increase, however, is less than the decrease, since the bearing is not loaded to the same extent by the second cylinder. The unloading caused

by the expansion in cylinder 2 is largely compensated for by the initial compression in cylinder 1. In the range of 180° to 240° crank angle the eccentricity changes only slightly. Only at about 215° crank angle is a short term eccentricity increase to be recorded for the measured curve. Between 240° and 360° crank angle, the relative eccentricity increases with increasing gas force in cylinder 1.

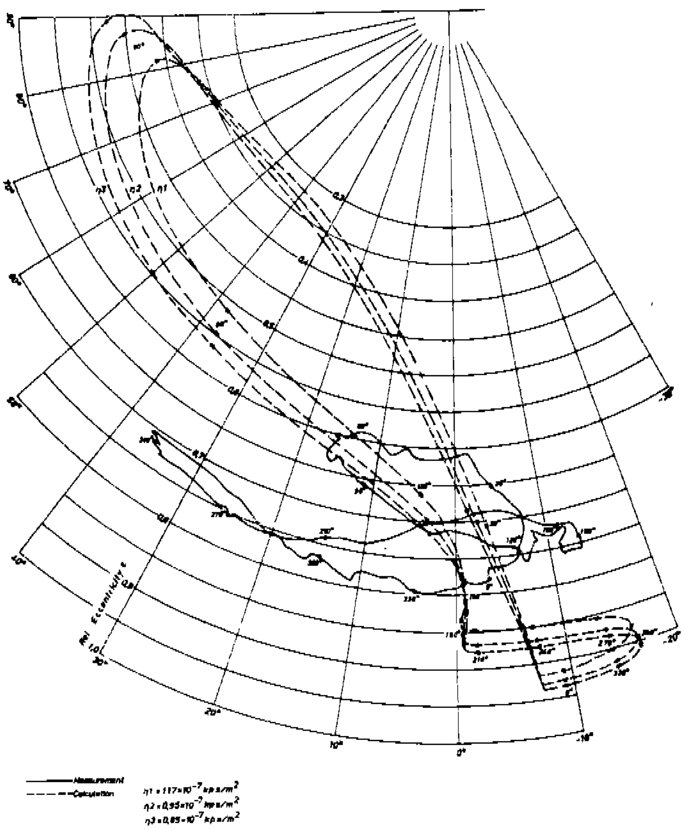

Fig. 7: Path motion

Apart from that, the measured and computed path motions show large differences. Between 0° and 180° the computed path motions show large variations of the relative eccentricity and simultaneously large angle movements, that is, the journal is moving rapidly in a radial as well as in an axial direction. The measured path shows the same tendency, however, with a remarkably smaller amplitude. The inertial forces of the oil apparently do not allow such large movement velocities as occur between 30° and 60° crank angle in the computation. In the range of 180° to 360° crank angle, the measured path motion takes a course which is opposite to that of the computation. An approximately conformity can only be established with maximum eccentricity.
One would have expected, however, that the relative eccentricity of the measured path was larger than that of the computed one with pure oil. Here the unpossibility of determining correctly the zero line in the measurement could be of particular relevance. A further possibility of error might be inaccuracy in determining the temperature, since the temperature was not measured in the lubrication film but in the bearing.
The computed paths, for which the viscosity was varied, show that the relative eccentricity increases with decreasing viscosity of the oil. In addition, one can observe a larger shift from the vertical of the smallest lubrication gap.
The computed and measured path movements when operating with R502 resemble those by operating with R12. Only in the range of 210° and 300° crank angle do we have vibrations for the measured path instead of large tangential movements. These vibrations can also be recognized in the bearing pressure recordings. They are possibly due to resonance vibrations in the lubrication film.
At the present stage of the investigations, relatively exact statements gained through computation can only be made on the size of the maximum eccentricity and its position (compare also Radermacher [6]).
The attempt to reach a conclusion on the actually existing lubricant viscosity in the bearing by means of a comparison of measured and computed paths, remains uncertain as long as it is impossible to determine the position of the shaft when the aggregate is at standstill.
The possibility of a comparison between measurement and computation is limited by the presuppositions made for the theory on the path motions, namely

1. Constant viscosity of the lubricant in the bearing
2. Rigidity of the shaft and bearing parts.

Appendix:

$$y = \frac{h_V}{H_V}$$ non dimensional valve lift

$$x = \frac{p_S - p}{p_S}$$ relative pressure difference at the suction valve

$$x = \frac{p - p_D}{p_D}$$ relative pressure difference at the discharge valve

Non dimensional parameters of the valve dynamic equation:

$$FVH = \left[\frac{n_F \cdot c_F}{m_V + n_F \cdot 0.3 \cdot m_F} \right]^{-0.5}$$

$$DFK = 0.5 \cdot C_D [n_F \cdot c_F (m_V + n_F \cdot 0.3 \cdot m_F)]^{-0.5}$$

$$VSP = \frac{F_O}{n_F \cdot c_F \cdot H_V}$$

$$ERG = \frac{C_{DR} \cdot A_{DR} \cdot p_{S,D}}{n_F \cdot c_F \cdot H_V}$$

Nomenclature:

A_{DR}	Area of valve face
A_Q	Area of flow in fully open valve
A_W	Surface for heat transfer
b	Width of the bearing
c_F	Spring stiffness per spring
c_m	Mean speed of piston
c_p	Specific heat at constant pressure
C_A	Coefficient of the heat transfer correlation
C_D	Damping factor
C_{DR}	Pressure drag coefficient
C_Q	Coefficient of discharge
C_R	Coefficient of restitution
d	Diameter of the bearing
D	Cylinder diameter
e	Eccentricity
F	Force acting on the bearing
F_D	Force caused by rotation only
F_V	Force caused by displacement only
F_O	Initial spring load per valve
h	Specific enthalpy
h_v	Variable valve lift
H	Gas enthalpy
H_V	Permitted valve lift
k	Exponent
m	Mass in the cylinder
m_F	Spring mass
m_V	Mass of valve plate
n	Revolutions per minute
n_F	Number of springs per valve
Nu	Nusselt-number
p_D	Pressure in the discharge chamber
p_S	Pressure in the suction chamber
P	Performance
Pr	Prandtl-number
Q_W	Heat transfered to cylinder walls because of heat exchange
r	Crank radius
R	Gas constant
Re	Reynolds-number
S	Stroke
So_D	Sommerfeld-number of rotation only
So_V	Sommerfeld-number of displacement only
t	Time
T	Gas temperature in the cylinder
T_W	Wall temperature
v	Specific volume
V	Cylinder volume
V_H	Cubic capacity
α	Heat transfer coefficient
β	Angle between force caused by rotation only and smallest lubrication gap
γ	Angle between force acting on the bearing and vertical
δ	Angle between smallest lubrication gap and vertical
ε	Relative eccentricity
ε_O	Relative clearance volume
η	Viscosity
κ	Isentropic exponent
λ	Thermal conductivity of the gas
λ_c	Quotient of connecting rod
ϕ	Crank angle
ψ	Relative bearings clearance
ω	Angular velocity of crank
ω_S	Angular velocity of bearing
$\bar{\omega}$	Effective angular velocity

Subscripts: S Suction- D Discharge- 0 Reference- 1 Upstream- 2 Valve-Conditions

	suction valve	discharge valve
dm > 0	Z = S	Z = D
dm < 0	without subscript	

References:

[1] Hahn, H.W., "Das zylindrische Gleitlager endlicher Breite unter zeitlich veränderlicher Belastung", Diss. Techn. Hochschule Karlsruhe (1957)

[2] Holland, J., " Beitrag zur Erfassung der Schmierverhältnisse in Verbrennungs-Kraftmaschinen", VDI-Forschungsheft 475 (1959)

[3] Eberhard, A. and Lang, O., " Zur Berechnung der Gleitlager im Verbrennungsmotor mittels elektronischer Digitalrechner", MTZ 22 (1961) Heft 7

[4] Gläser, H., " Berechnung der Radiallager von Kältemittelkompressoren", Zeitschr. Luft- und Kältetechnik Heft 6 (1971), Heft 1 (1972), Heft 2 (1972), Heft 4 (1972)

[5] Fränkel, A., "Berechnung von zylindrischen Gleitlagern", Diss. Eidgen. Techn. Hochschule Zürich (1944)

[6] Radermacher, K.H., "Das instationär belastete Gleitlager", Diss. Techn. Hochschule Karlsruhe (1962)

[7] Ashrae Guide and Data Book, Equipment, New York 1969

[8] Barho, W., "Die Molwärme der Fluor-Chlor-Derivate des Methans im Zustand idealer Gase", Kältetechnik 17 (1965) Heft 7

[9] Zapf, H., "Untersuchung des Wärmeübergangs in einem Viertakt-Dieselmotor während der Ansaug- und Ausschubperiode", MAN Forschungsheft 14 (1968/69)

[10] Woschni, G., "Die Berechnung der Wandverluste und der thermischen Belastung der Bauteile von Dieselmotoren", MTZ 31 (1970) Nr. 12

[11] M.Wambsganss, R.Cohen, "Dynamics of a reciprocating compressor with automatic reed valves. Theory and Simulation". XII International Congress of Refrigeration, August/September, 1967, Madrid